Industrial Crops & Products 126 (2018) 103–112

Contents lists available at ScienceDirect

Industrial Crops & Products

journal homepage: www.elsevier.com/locate/indcrop

Improved application of natural forest product terpene for discovery of potential botanical fungicide

Yanqing Gao[a,1], Yong Wang[a,1], Jian Li[b,*], Shibin Shang[c], Zhanqian Song[c]

[a] College of Plant Protection, Northwest A&F University, Yangling, Shaanxi 712100, People's Republic of China
[b] College of Forestry, Northwest A&F University, Yangling, Shaanxi 712100, People's Republic of China
[c] Institute of Chemical Industry of Forest Products, Chinese Academy of Forestry, Nanjing, Jiangsu 210042, People's Republic of China

ARTICLE INFO

Keywords:
Terpene
Acyl-thiourea
Antifungal activity
Biochemical response
QSAR

ABSTRACT

The development of efficient terpenoid fungicides and exploration of its action mechanism is of great significance for the prevention and control of agricultural diseases. To confirm our previous findings on naturally occurring antifungal products with ecofriendly features, 40 terpene-based acyl-thiourea derivatives were synthesized and structurally characterized by ^{1}H NMR, ESI-MS, elemental analysis and IR spectroscopy. Their inhibitory activities against several fungi, including *Botrytis cinerea*, *Sclerotinia sclerotiorum* and *Thanatephorus cucumeris*, were assessed by the growth rate method and the *in vivo* antifungal effects of these compounds against *Thanatephorus cucumeris* were performed evaluated using detached leaves. The majority of these compounds showed moderate to marked antifungal activities. Of all compounds, myrtenyl-based acylthiourea (8i) displayed more pronounced antifungal activity against *Thanatephorus cucumeris* (EC_{50} = 0.412 mg/L) compared with carbendazim (EC_{50} = 0.436 mg/L). *In vivo* antifungal of compound 8i efficiency against *Thanatephorus cucumeris* was also excellent. Treatment with 8i of *Thanatephorus cucumeris* resulted in significantly influenced morphology, markedly increased cell membrane permeability, and reduced ATP amounts and ATPase activity in comparison with untreated controls. A total of four descriptors linking structures and antifungal activities against *Thanatephorus cucumeris* were determined, including q^{S}_{max}, *HOMO-LUMO*, log *MS* and q^{N}_{max}, and employed to build a quantitative structure-activity relationship (QSAR) model (R^2 = 0.9673). Preliminary structure-activity relationship (SAR) and QSAR assessments revealed that electronic and steric effects as well as energy differences of various molecules markedly affected antifungal effects. These findings provide novel insights into the modes of action of terpene-based acyl-thiourea derivatives, which could constitute potential substitutes for current fungicides or leads for novel antifungal agent development.

1. Introduction

In the modern agriculture, the management of harmful organisms needs more integrated consideration (Sparks Thomas et al., 2016). At the same time of crop protection against plant diseases, the public health problem and food safety issue should be considered equally (Gao et al., 2015). Compared with the single synthesized fungicide, the new antifungal drugs of novel structure, low cost and high efficient activity can eliminate some adverse consequences, such as the development of resistance, side effects to the environment non-target organisms, and have better prospects for exploitation. As a feasible solution, the rational application of renewable and abundant natural products to develop of new fungicides is an essential factor in the modern agricultural industry (Smith et al., 2018). The increasing demand for agrochemical products with high performances requires modification of natural products (Sparks Thomas et al., 2016). Terpenes constitute the largest class of natural products, and inhibit several infectious organisms, including viral, bacterial, fungal, protozoal and parasitic agents (Wright et al., 2001; Ntalli et al., 2010; James Bound et al., 2016; Kiyama, 2017). As inexpensive, abundant, and renewable materials, terpenes and terpene-based derivatives continue to influence modern agricultural industry (Smith et al., 2018; Zhao et al., 2018). On the other hand, introduction of bioactive scaffolds may improve the biochemical properties of the original natural products, increasing the efficacy of these molecules (Jenkins et al., 2008; Quin et al., 2014; Zhang et al., 2017).

Acyl-thiourea derivatives are endowed with widespread biological activities, including insecticidal, antiviral, antibacterial, herbicidal,

* Corresponding author.
E-mail address: ericlee99@nwsuaf.edu.cn (J. Li).
[1] The authors contributed equally to this work and should be considered co-first authors.

https://doi.org/10.1016/j.indcrop.2018.10.008
Received 5 August 2018; Received in revised form 25 September 2018; Accepted 2 October 2018

plant growth regulating effects. Recently, acyl-thiourea products have attracted increasing attention in crop protection as antifungal agents (Burgeson et al., 2012; Solinas et al., 2012; Zhang et al., 2012; Wang et al., 2014; Yun et al., 2016). Meanwhile, related studies uncovered that oxygen, nitrogen and sulfur donor hetero-atoms might be crucial for the antifungal activity, providing a number of multiple reactive sites conferring inhibitory effects against fungi (Yang et al., 2017; Joshi et al., 2018). We previously reported that rosin-based acyl-thiourea compounds show remarkable agricultural activity (Gao et al., 2015). Therefore, to broaden the activity and develop of new antifungal agents with higher activity and lower toxicity, the acyl-thiourea scaffold was incorporated into terpene structures.

Then, to introduce the acyl-thiourea group into the terpene structure and assess its effects on antifungal activity, we selected the abundant renewable terpenoid resource pine resin, as a starting point to synthesize terpene-based acyl-thiourea derivatives. Four acyl-thiourea compounds, namely acrylpimaric and dehydroabietic (rosin derivatives, two terpenoids), dihydrocumatyl and myrtenyl (turpentine derivatives, monoterpenes) acyl-thiourea compounds were prepared by nucleophilic acylation between aroylisothiocyanates and amines. Their antifungal activities against *Botrytis cinerea*, *Sclerotinia sclerotiorum* and *Thanatephorus cucumeris* were tested accordingly. In order to improve study efficiency and reduce cost, the QSAR methodology as an essential tool was applied to screen the active compounds effectively, identify the molecular features of terpene-based acyl-thiourea derivatives responsible for antifungal activity, and deduce potential target sites (Papa et al., 2010). Some physicochemical properties related to activity such as spatial structure, molecular size, effect of water solubility, group polarity, and electron donating/accepting capability were assessed by biochemical response and structure-activity relationship studies. Our findings are expected to improve the application of terpenes as antifungals.

2. Materials and methods

2.1. Compound synthesis and characterizations

Different compounds were assessed by FT-IR spectroscopy on a Nicolet IS10 Fourier transform infrared spectrophotometer (Thermo Nicolet Co., Madison, USA). ^{1}H NMR spectrometry was carried out on a Bruker AV-300/500 (300/500 MHz) spectrometer with tetramethylsilane as an internal reference; ESI mass spectrometry was performed on a Bruker Q-TOF mass spectrometer (Bruker Co., Karlsruhe, Germany). Elemental analysis was carried out on a Vario EL-III (Elementar Co., Hanau, Germany). Chemically pure reagents were employed, except for crude rosin and β-pinene, obtained from Wuzhou Pine Chemicals. Reactions were monitored by thin layer chromatography (TLC). Four series of acyl-thiourea derivatives were prepared through nucleophilic acylation reaction between terpene-based carboxylic acids and amines, which were shown in Schemes 1 and 2.

2.1.1. Synthesis of terpene-based carboxylic acids

Following the procedures described in our previous reports (Li et al., 2016; Liao et al., 2017), dehydrocumic acid (**2, DHA**) was prepared through alkaline potassium permanganate oxidation and dehydration rearrangement reactions, respectively, from β-pinene. Meanwhile, myrtanol (**4**) was prepared *via* hydroboration-oxidation reaction from β-pinene, and submitted to chromic acid oxidation reaction to yield myrtanic acid (**5, MRA**).

In order to prepare rosin-based acyl-thiourea, two rosin-based carboxylic acids were synthesized. Dehydroabietic acid (**9**, **DHAA**) was prepared through disproportionation reaction from rosin catalyzed by Pd/C (Gao et al., 2013). Meanwhile, rosin-based dicarboxylic acid (**10**, **APA**) was synthesized through Diels-Alder addition involving rosin with acrylic acid (Gao et al., 2015).

2.1.2. Synthesis of terpene-based carbonyl chloride

The above synthesized terpene-based carboxylic acids were used prepare terpene-based carbonyl chlorides. The specific steps were as follows. In a 250 mL flask equipped with water-cooled condenser, thermometer, drying tube and dropping funnel, the terpene-based carboxylic acid (10 mmol) was dissolved in CH_2Cl_2 (80 mL). Then, thionyl chloride (2.38 g, 20 mmol) was added dropwise within 1 h and refluxed for 4 h at 65 °C. Dihydrocumatyl chloride (**3**), myrtanyl chloride (**6**), and dehydroabietyl chloride (**11**) were obtained as yellowish oily products after solvent and complete thionyl chloride removal. Meanwhile, **APA** (3.75 g, 10 mmol) in the above-mentioned method reacted with thionyl chloride (4.76 g, 40 mmol) to yield the target compound acrylpimaryl chloride (**12**), also as yellowish oil.

2.1.3. Synthesis of terpene-based acyl-thiourea compounds

KSCN solution (0.97 g, 10 mmol), terpene-based carbonyl chloride (10 mmol) and 100 mL anhydrous CH_3CN were mixed in a 250 mL flask equipped as described above. After reaction (24 h, 70 °C), the product was filtered and tested with no further purification. This was followed by organoamine (10 mmol) addition and reflux for 2 h. Dihydrocumatyl (**7a-j**), myrtenyl (**8a-j**), and dehydroabietic (**13a-j**) acyl-thiourea compounds were obtained after drying with anhydrous $MgSO_4$ and purification by silica gel chromatography, with ethyl acetate/petroleum ether (1:10) as eluent. Moreover, acrylpimaric acyl-thiourea derivatives (**14a-j**) were prepared by adopting the above-mentioned methods and acrylpimaryl chloride (**12**) (4.11 g, 10 mmol) reacted with KSCN (1.94 g, 20 mmol) and organoamine (20 mmol) in acetonitrile solution. Schemes 1 and 2 **s**how the synthetic routes and structural representations of the target compounds **7a-j** and **8a-j**, **13a-j** and **14a-j**.

2.2. Biological assays

First of all, it was performed the antifungal activity of terpene-based acyl-thiourea derivatives against *B. cinerea*, *S. sclerotiorum* and *T. cucumeris* by the growth rate method and the *in vivo* antifungal effects of these compounds against *T. cucumeris* were performed evaluated using detached leaves. The morphological properties of *T. cucumeris* mycelium were assessed on an S-3400 N scanning electron microscope (SEM) (Hitachi, Tokyo, Japan). Conductivity was measured on a CON510 Eutech/Oakton conductivity meter (OAKTON Instruments, Vernon Hills, USA). ATP levels and ATPase activity were measured with commercially available kits (Jiancheng Bioengineering Instruments, Nanjing, China) as directed by the respective manufacturers.

2.2.1. Antifungal activity test by the growth rate method

Preliminary antifungal activities of the terpene-based acyl-thiourea derivatives were determined by the growth rate method against three fungi, including *B. cinerea*, *S. sclerotiorum* and *T. cucumeris* (Gao et al., 2015). Carbendazim was assessed as a positive control. The tested chemicals were dissolved in anhydrous methanol/sterile water with Tween-80 (1 mL/L) to yield a stock solution at a concentration of 10 g/L, which was diluted with melted culture medium to 100, 50, 25, 12.5 and 6.25 mg/L, respectively. Then, the tested pathogens were inoculated on pastille tablets which were poured on medicated media and placed in a constant temperature incubator. The same amounts of anhydrous methanol/sterile water with Tween-80 solution served as negative control. Colony diameters for the tested chemicals were measured by calipers in mm when the colony diameter reached 50–60 mm in the negative control. Triplicate tests were performed. Inhibition rates (*IR*) were employed to evaluate the antifungal effects of various compounds as shown in Eq. (1):

$$IR\ (\%) = (C - T)/\ (C - 5) \times 100 \quad (1)$$

where C and T are diameters of control and treated colonies, respectively. EC_{50} value for each chemical was calculated by regression

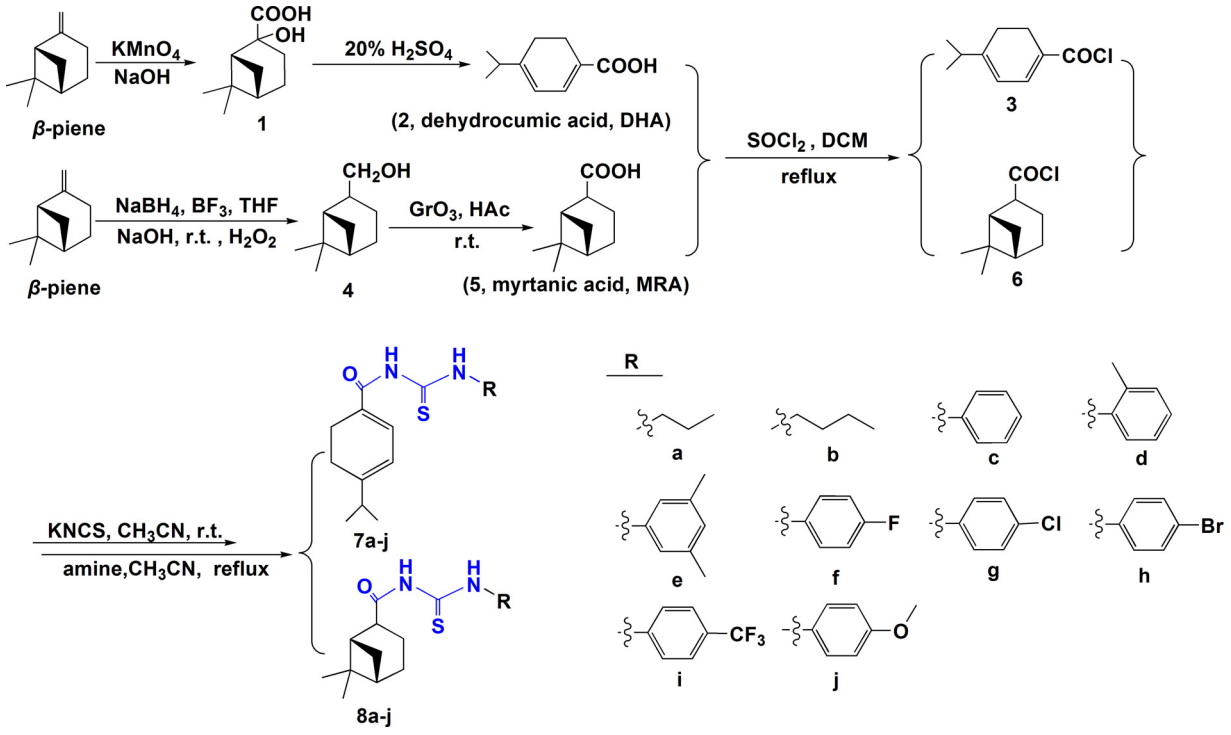

Scheme 1. Synthesis route of pinene-based acyl-thiourea compounds.

analysis with the SPSS software according to the concentration corresponding to *IR* results, and values in columns followed by similar letters were not significantly different according to Fisher's protected LSD test ($P = 0.05$) (Yun et al., 2015).

2.2.2. In vivo antifungal effects of test products against T. cucumeris

Terpene-based acyl-thiourea derivatives possessing good antifungal effects against *T. cucumeris* were further evaluated using detached leaves (Jing et al., 2014; Yu et al., 2018). The tested chemicals were dissolved in anhydrous methanol/sterile water with Tween-80 (5 mL/L)

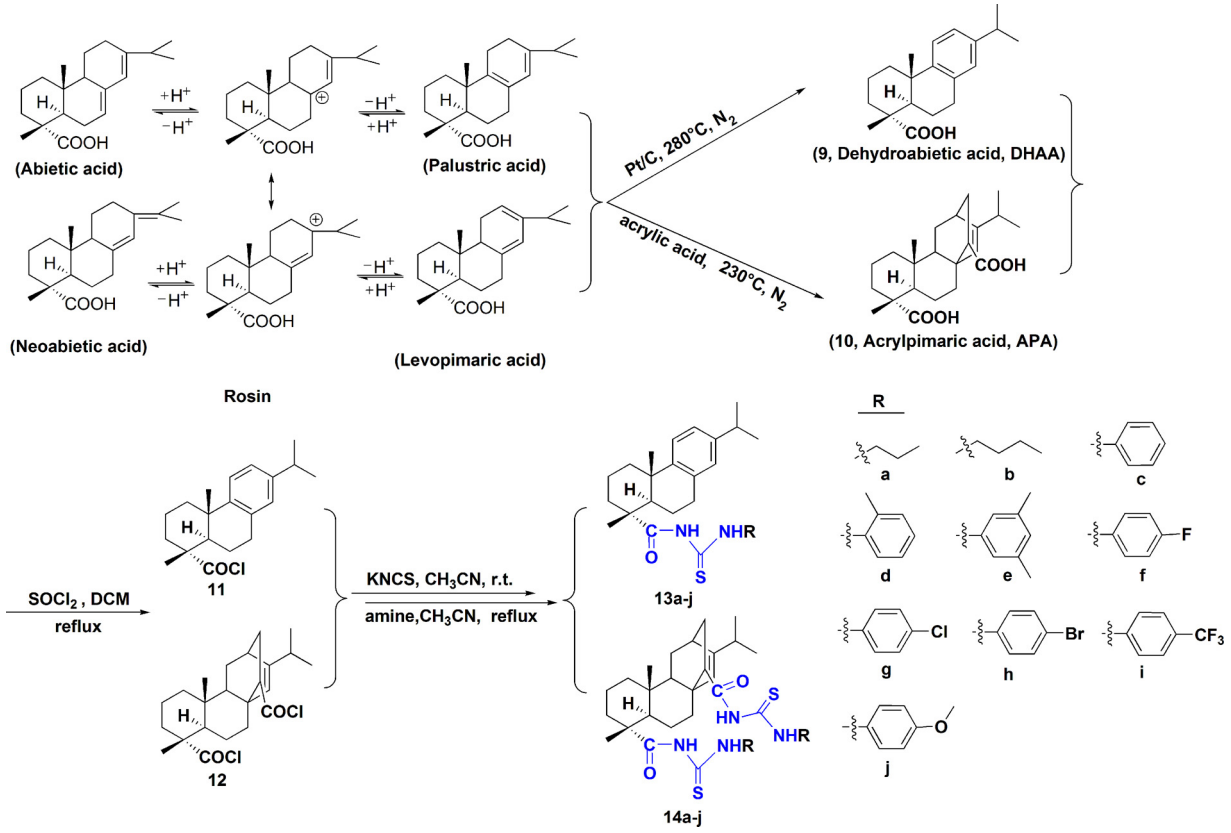

Scheme 2. Synthesis route of rosin-based acyl-thiourea compounds.

to yield different concentrations, including 100, 50, and 25 mg/L, respectively. Leaves with the same position and consistent growth on the potted pea seedlings were cut and moistened. Then, they were sprayed with the above solutions and air dried. Next, the hyphae side of *T. cucumeris* was attached to the center of the foliage and moved into an illuminated culture room at a temperature of 26–28 °C for inoculating and five days of growth. The extent of lesion expansion at each inoculation site was measured by calipers. The control effect (*CE*) was employed to assess antifungal effects against *T. cucumeris*, and determined as in Eq. (2):

$$CE\ (\%) = (Cs - Ts)/\ (Cs - 5) \times 100 \quad (2)$$

where *Cs* and *Ts* are lesion expansion sums of control and treated lesions, respectively.

2.2.3. Effect of the MRA-based acyl-thiourea (8i) on mycelial morphology in T. cucumeris

Mycelial plugs excised from the margins of 4 day old colonies were placed side down on PDA plates supplemented with 2 mg/L of the MRA-based acyl-thiourea compound (**8i**) (Lv et al., 2017). Plates without 8i constituted negative controls. The samples were incubated for 2 days at 25 °C away from light, the medium margins (10 mm × 10 mm) were obtained and placed on glass slides. The morphological properties of *T. cucumeris* mycelium after treatment with the test compound (**8i**) were assessed under a SEM. Two triplicate experiments were carried out.

2.2.4. Effect of the MRA-based acyl-thiourea (8i) on cell membrane permeability

Ten mycelial plugs of *T. cucumeris* were cultured in 100 mL PDA (Berben et al., 2018), with shaking (175 rpm) and 25 °C for 3 days, followed by treatment without or with **8i** (2 mg/L) for another day. Then, 0.5 g of fresh mycelia was resuspended in 25 mL distilled water, whose conductivity was assessed at 1, 2, 4, 6, 8, 10 and 12 h, respectively, on a conductivity meter. Afterwards, final conductivity was obtained after mycelial boiling for 5 min. Three triplicate experiments were performed. Relative conductivity was derived as in Eq. (3):

$$\text{Relative conductivity (\%)} = \text{Conductivity at different times/Final conductivity} \times 100 \quad (3)$$

2.2.5. ATP levels and ATPase activity

ATP amounts (mmol/mg protein in the tissue) and ATPase activity (1 μmol inorganic phosphorus catalyzed in 1 mg protein in 1 h or μmol Pi/mg pro/h) in the *T. cucumeris* mycelium were assessed as previously reported (Sklenar et al., 1994; Shao et al., 2015). Two triplicate experiments were performed.

2.3. Building a QSAR model

The QSAR of antifungal activity for terpene-based acyl-thiourea derivatives was assessed with the quantum chemistry software according to previously reported methods (Gao et al., 2015). Briefly, conformer optimization and minimum energy calculation were carried out at the 6-31 G (d) level through the density functional theory using the Gaussian 16 software (Gaussian, Inc., wallingford, USA). Data format was converted with the Ampac 9.1.3 program (Semichem Inc. Shawnee, USA) for compatibility with the CODESSA 2.7.15 software (Semichem Inc. Shawnee, USA) for the assessment of descriptors. Meanwhile, the best multiple-liner regression (BMLR) analysis approach was selected by CODESSA 2.7.15 for building a QSAR model. EC_{50} values for test compounds in *T. cucumeris* were log transformed to better correlate activity and descriptors. The final QSAR model with good regression between log EC_{50} and various descriptors could interpret the effects of the structural features of terpene-based acyl-thiourea derivatives on fungi. Furthermore, the "leave-one-out" cross-validation and internal validation approaches were employed to generate the QSAR model.

3. Results and discussion

3.1. Terpene-based acyl-thiourea derivatives prepared

The turpentine-based carboxylic acids, dehydrocumic acid (**2, DHA**) and myrtanic acid (**5, MRA**) were prepared mainly through oxidation reactions from *β*-pinene. Meanwhile, rosin-based carboxylic acids (**9**, **DHAA** and **10**, **APA**) were obtained principally *via* disproportionation reaction or Diels-Alder addition reaction from rosin. The above-mentioned terpene-based carboxylic acids were reacted with thionyl chloride to yield the corresponding pinene-based carbonyl chloride (**3**, **6**) and rosin-based carbonyl chloride (**11, 12**). The terpene-based acyl-thiourea analogues **7a-j**, **8a-j**, **13a-j** and **14a-j** were obtained from carbonyl chloride reaction with potassium thiocyanate and aliphatic and aromatic amines in the CH_3CN solution *via* a convenient two step reaction. The intermediate acyl isocyanate was tested with no further purification. As acyl-thiourea compounds had stable amide group structures, reaction yields were correspondingly high (60–77%).

3.2. Antifungal activity and biochemical response

3.2.1. Antifungal activity against T. cucumeris and structure-activity relationship

The terpene-based acyl-thiourea derivatives synthesized exhibited reduced fungicidal activities against *B. cinerea* and *S. sclerotiorum* in comparison with *T. cucumeris*, and inhibition rates were generally below 20% at 100 μg/mL. The antifungal activities of various compounds against *T. cucumeris* are listed in Table 1, which indicates moderate to significant antifungal activities, and values in columns followed by similar letters were not significantly different according to Fisher's protected LSD test ($P = 0.05$) (Yun et al., 2015).

Although an overt structure-activity relationship from Table 1 seems challenging, we can be concluded clearly that turpentine-based compounds (**7a-j** and **8a-j**) exhibited obviously higher activities compared with rosin-based counterparts (**13a-j** and **14a-j**) with the same substituted group. MRA-based acyl-thiourea compounds (**8a-j**) exhibited similar antifungal activities to the control carbendazim. Even at 1.56 mg/L, compounds **8c-i** still displayed significant antifungal activities against *T. cucumeris* (> 75% inhibition). It is worth noting that **8f-g** showed inhibition rates of 91.80–93.60% at 6.25 mg/L and 75.44–76.00% at 3.13 mg/L, indicating equality or superiority to carbendazim (91.65% and 75.44% inhibition at 6.25 mg/L and 3.13 mg/L, respectively) against *T. cucumeris*. The EC_{50} values of these four compounds were 0.447, 0.522, 0.595, and 0.412 mg/L respectively, which were similar to carbendazim (EC_{50} of 0.436 mg/L). In particular, compound **8i** had a lower EC_{50} value compared with carbendazim. These findings demonstrated that antifungal activity differences were caused by variations in combinations of terpene-based backbone structure and active substructures.

SAR and QSAR reports suggested electronic and steric effects of substituent groups are critical for the biological properties of terpene derivatives (Baba and Yoshioka, 2009; Yoshioka and Baba, 2009; Deb et al., 2014; Thiehoff et al., 2016; Curtin et al., 2017). Table 1 shows that while compounds possessing aliphatic chains and electron-donating substituents (methoxy groups) in the aromatic ring, which displayed low antifungal activities, the majority of chemicals with the electron-withdrawing substituents F, Cl, Br, and -CF_3 showed elevated antifungal activities against *T. cucumeris* in the same series (*e.g.*, **7f-i** > **7c-e** > **7a**, **7b** > **7 j**; **8f-i** > **8c-e** > **8a**, **8b** > **8 j**, *etc.*). These findings suggested substitution patterns on the benzene ring significantly affect the antifungal activities of terpene-based acyl-thiourea moieties. Meanwhile, DHA and MRA-based acyl-thiourea compounds possessed smaller volumes in spatial structure compared with DHAA and APA-

Table 1
Antifungal activities of terpene-based acyl-thiourea compounds against *T. cucumeris*.

Compound	*IR* (%) at a concentration of (mg/L)										
	100.00	50.00	25.00	12.50	6.25	3.13	1.56	0.78	EC_{50}	$y = a + bx$	log EC_{50}
7a	100.00	88.00	72.00	60.30	53.10	47.60	42.50	40.80	6.401f	$y = -0.307 + 0.051x$	0.806
7b	100.00	88.00	72.50	61.00	53.90	48.30	43.00	41.90	5.438f	$y = -0.274 + 0.050x$	0.735
7c	100.00	89.20	75.80	62.80	55.23	50.35	46.18	44.85	3.483g	$y = -0.178 + 0.051x$	0.542
7d	100.00	89.15	76.10	62.75	55.20	50.25	46.20	44.90	3.476g	$y = -0.178 + 0.051x$	0.541
7e	100.00	89.20	75.10	60.80	55.10	49.60	45.50	44.90	3.476g	$y = -0.205 + 0.051x$	0.541
7f	100.00	100.00	99.00	89.50	70.50	66.20	48.40	40.50	1.635h	$y = -0.334 + 0.204x$	0.214
7 g	100.00	100.00	99.20	89.60	70.25	65.00	49.10	41.00	1.648 h	$y = -0.339 + 0.205x$	0.217
7 h	100.00	100.00	99.20	89.60	70.25	65.00	49.10	41.50	1.614 h	$y = -0.330 + 0.205x$	0.208
7i	100.00	100.00	99.00	89.50	70.30	65.20	49.20	41.50	1.575h	$y = -0.317 + 0.201x$	0.197
7 j	100.00	86.00	71.00	60.00	51.50	45.80	42.80	40.50	6.719f	$y = -0.327 + 0.049x$	0.827
8a	100.00	98.00	82.50	66.80	59.23	52.35	48.18	44.85	2.601gh	$y = -0.196 + 0.075x$	0.415
8b	100.00	98.50	82.00	67.00	59.00	51.30	48.20	45.00	2.777 gh	$y = -0.213 + 0.077x$	0.443
8c	100.00	100.00	100.00	99.00	90.00	74.00	59.00	48.00	0.754i	$y = -0.308 + 0.408x$	−0.123
8d	100.00	100.00	100.00	98.50	90.00	75.20	58.60	46.00	0.823i	$y = -0.336 + 0.408x$	−0.085
8e	100.00	100.00	100.00	99.50	90.50	76.20	58.40	46.50	0.887i	$y = -0.401 + 0.453x$	−0.052
8f	100.00	100.00	100.00	99.10	92.50	75.44	60.20	54.20	0.447i	$y = -0.187 + 0.417x$	−0.350
8 g	100.00	100.00	100.00	99.20	91.80	75.50	60.00	52.80	0.522i	$y = -0.219 + 0.419x$	−0.282
8 h	100.00	100.00	100.00	99.30	91.80	76.00	60.00	51.50	0.595i	$y = -0.257 + 0.432x$	−0.225
8i	100.00	100.00	100.00	99.60	93.60	75.44	61.00	56.20	0.412i	$y = -0.182 + 0.442x$	−0.385
8 j	100.00	88.00	72.50	60.50	53.90	47.50	43.00	40.50	5.845f	$y = -0.298 + 0.051x$	0.768
13a	95.00	78.00	55.00	40.50	32.00	18.00	/	/	24.356d	$y = -1.127 + 0.046x$	1.387
13b	95.00	77.50	54.80	40.20	31.80	17.90	/	/	24.626d	$y = -1.135 + 0.046x$	1.391
13c	98.00	84.00	71.00	46.00	41.00	34.50	27.00	/	14.980e	$y = -0.785 + 0.052x$	1.176
13d	98.00	83.50	72.00	46.50	40.60	34.00	26.00	/	14.963e	$y = -0.787 + 0.053x$	1.175
13e	98.00	83.10	72.00	46.50	40.60	34.00	25.80	/	15.199e	$y = -0.798 + 0.052x$	1.182
13f	99.00	89.00	72.00	59.00	49.50	42.00	28.00	/	13.539e	$y = -0.965 + 0.071x$	1.131
13 g	99.00	89.50	72.90	59.30	49.20	42.80	28.20	/	13.244e	$y = -0.961 + 0.073x$	1.122
13 h	99.20	89.50	73.10	59.50	49.50	42.80	28.50	/	13.090e	$y = -0.962 + 0.073x$	1.117
13i	99.00	89.20	71.80	59.00	49.00	42.50	28.00	/	13.532e	$y = -0.967 + 0.071x$	1.131
13 j	90.50	65.00	44.30	37.50	22.00	/	/	/	33.101c	$y = -1.167 + 0.035x$	1.520
14a	85.00	56.00	39.00	31.60	18.00	/	/	/	42.777b	$y = -1.354 + 0.032x$	1.631
14b	85.50	56.20	38.50	30.90	18.50	/	/	/	42.647b	$y = -1.371 + 0.032x$	1.630
14c	90.40	65.00	46.00	38.80	22.00	/	/	/	32.294c	$y = -1.119 + 0.035x$	1.509
14d	90.20	65.00	45.80	38.00	22.00	/	/	/	32.645c	$y = -1.132 + 0.035x$	1.514
14e	90.50	64.00	41.00	35.60	22.00	/	/	/	34.855c	$y = -1.246 + 0.036x$	1.542
14f	97.00	82.10	75.00	40.00	35.00	30.00	25.80	/	17.402e	$y = -0.922 + 0.053x$	1.241
14 g	97.00	81.80	75.40	40.50	35.00	30.00	25.50	/	17.363e	$y = -0.918 + 0.053x$	1.239
14 h	97.00	82.00	75.00	40.50	35.00	30.00	25.50	/	17.388e	$y = -0.921 + 0.053x$	1.240
14i	97.00	82.10	75.80	40.50	35.00	30.00	25.50	/	17.241e	$y = -0.918 + 0.053x$	1.237
14 j	77.00	43.50	22.00	15.00	8.00	/	/	/	62.382a	$y = -2.230 + 0.036x$	1.795
Carbendazim	100.00	100.00	100.00	99.50	91.65	75.44	60.80	54.40	0.436i	$y = -2.208 + 0.034x$	

Values in columns followed by similar letters were not significantly different according to Fisher's protected LSD test (P = 0.05).

based counterparts as shown in Schemes 1 and 2. As shown in Table 1, compounds **7a-j** and **8a-j** exhibited slightly higher activities in comparison with the **13a-j** and **14a-j** compounds with the same substituent. When $-OCH_3$ was added to the benzene ring, activities were comparably reduced, suggesting large side chains in this position had negative effects on activity. Therefore, we speculated that different terpene-based backbone structure or substitution patterns on the benzene ring play critical roles in the activity of terpene-based acyl-thiourea compounds against *T. cucumeris*.

3.2.2. *In vivo antifungal activity of the MRA-based acyl-thiourea (**8i**) against T. cucumeris*

The MRA-based acyl-thiourea compound (**8i**) showed good antifungal effects comparable to carbendazim. CE values were 91%, 80%, 60% at the concentrations of 100, 50, 25 mg/L, respectively. The *in vivo* antifungal activity of the MRA-based acyl-thiourea compound (**8i**) against *T. cucumeris* was experimentally evaluated in a greenhouse and shown in Fig. 1**a-h**.

3.2.3. *Effect of the MRA-based acyl-thiourea (**8i**) on mycelial morphology*

The ultrastructure of *T. cucumeris* mycelia after treatment with **8i** was assessed by SEM; at 1.0 μg/mL **8i**, severe mycelial deformation was observed, with folded mycelial surface, while untreated plates showed natural structure (Fig. 2**a–d**).

3.2.4. *Effects on cell membrane permeability*

The relative conductivity of the *T. cucumeris* mycelium increased over time in both **8i** and control groups (Fig. 3). However, **8i** treatment resulted in increased cell membrane permeability compared with untreated controls at all-time points. After 10 h, relative conductivity was stable. These findings indicated the MRA-based acyl-thiourea (**8i**) may cause cell membrane damage and enhance electrolyte leakage in the *T. cucumeris* mycelium. Upon treatment with **8i**, mycelial morphology was markedly altered, likely causing structural damage. Meanwhile, enhanced electrolyte leakage might result in elevated relative conductivity of the mycelium. According to previous reports, acyl-thiourea compounds could exert antifungal effects by causing fungal cell membrane defects (Sun et al., 2006; Haynes et al., 2014; Manetti et al., 2015). The above findings suggested that the action site of MRA-based acyl-thiourea compounds in *T. cucumeris* may be the cell membrane.

3.2.5. *ATP amounts and ATPase activity*

ATP represents the direct energy source in all living organisms (Sklenar et al., 1994; Shao et al., 2015), and ATPase activity indicates the rate of energy utilization (Tsuchikawa et al., 2016; Yang and Wang, 2016; Schwamborn et al., 2017; Sekiya et al., 2018). Upon culture in presence of the MRA-based acyl-thiourea (**8i**), ATP levels were markedly reduced in comparison with control values (Fig. 4a). The same trend was observed for ATPase activities (Fig. 4b). These findings

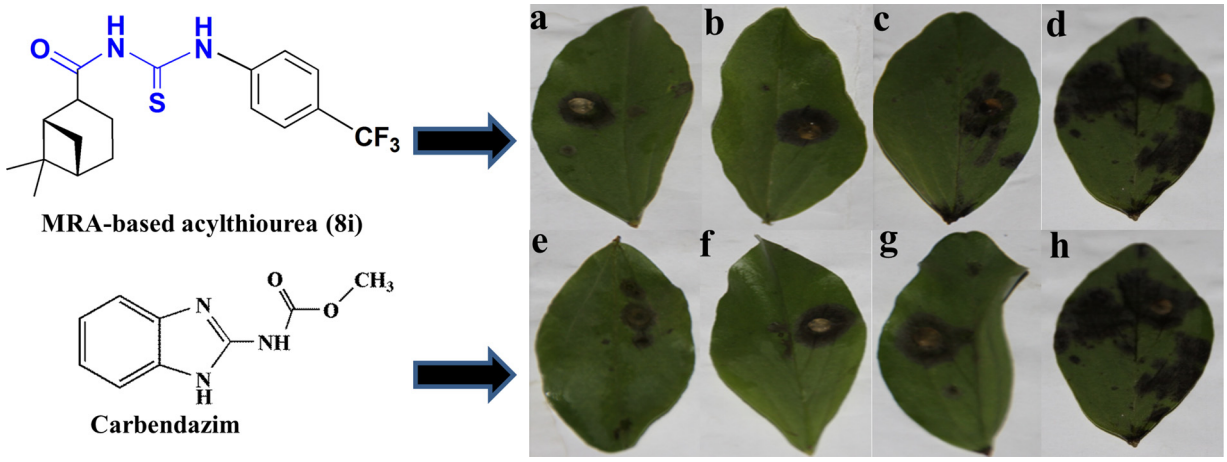

Fig. 1. Antifungal activity evaluated using *in vitro* leaf treated with MRA-based acyl-thiourea (8i) and carbendazim, respectively. a, e: 100 μg/mL; b, f: 50 μg/mL; c, g: 25 μg/mL; d, h: CK.

indicated that **8i** decreases ATPase activity and inhibits energy production in *T. cucumeris*.

3.3. Quantitative structure-activity relationship assessment of antifungal activity against T. cucumeris

The best regression relation between structure descriptors of terpene-based acyl-thiourea compounds and antifungal activity against *T. cucumeris* were established as reported previously (Gao et al., 2015). At this present work, 40 synthesized terpene-based acyl-thiourea derivatives and six groups of molecular descriptors were selected as samples and assessed. The best multiple linear regression analysis was chosen for constructing the QSAR model. The four descriptors attributed to the antifungal activities of molecular structures were confirmed using the "breaking point" graph rule (Fig. 5a). The four descriptors and obtained results are presented in **Table A. 1** and Table 2 according to their statistical importances.

The internal validation and "leave-one-out" cross-validation methods were employed for the validation of the built model according to a previously reported method (Vraćko et al., 2004; Song et al., 2013). In internal validation, the obtained 40 compounds were assigned to the A, B, and C groups, respectively. Compounds **7a**, **7d**, **7 g**, **7 j**, **8c**, **8f**, **8i**, **13b**, **13e, 13 h, 14a, 14d, 14 g** and **14 j** were classified under subset (A); **7b**, **7e**, **7 h**, **8a**, **8d**, **8 g**, **8 j**, **13c**, **13f, 13i, 14b, 14e** and **14 h** were under subset (B), and **7c**, **7f**, **7i**, **8b, 8e**, **8 h**, **13a**, **13d, 13 g, 13 j, 14c, 14f** and **14i** belonged to group (C). Two of the three subsets (A + B, A + C and B + C) were considered the training set, with the remaining group serving as the test set. Various training sets were employed to generate correlation equations based on the above mentioned descriptors in the final QSAR model; prediction of the corresponding values for the validation set was then performed using the established equations. Table 3 shows internal validation results, with mean R^2_{Training}

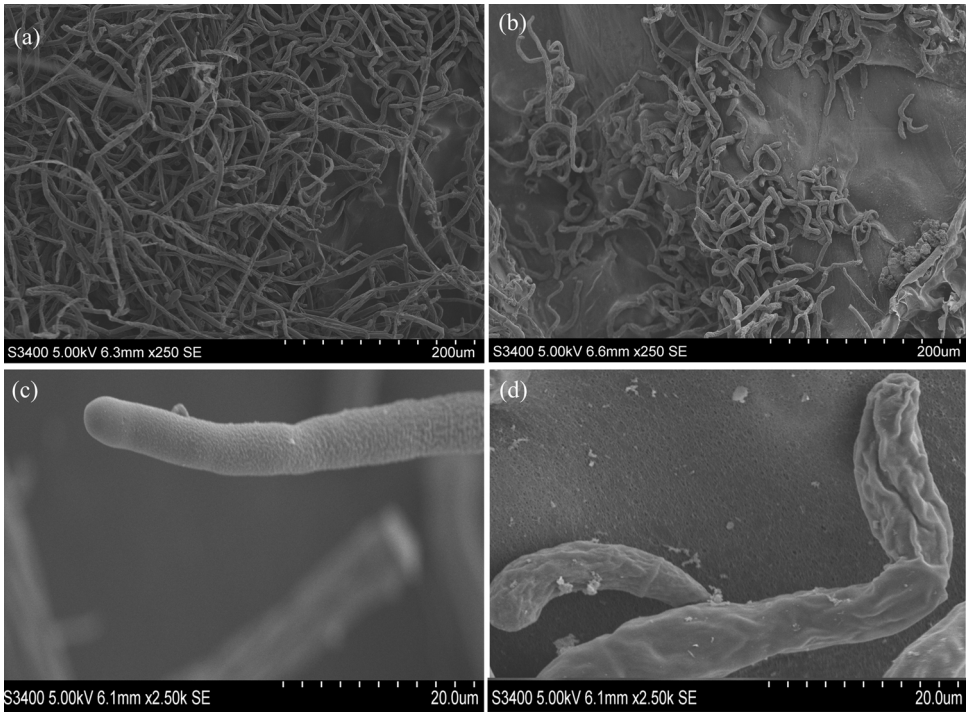

Fig. 2. Effect of the MRA-based acyl-thiourea (8i) on mycelial morphology in *T. cucumeris*. (a, b): 250 times, plates untreated and treated with 1 μg/mL (8i); (c, d): 2.50 K times, plates untreated and treated with 1 μg/mL (8i).

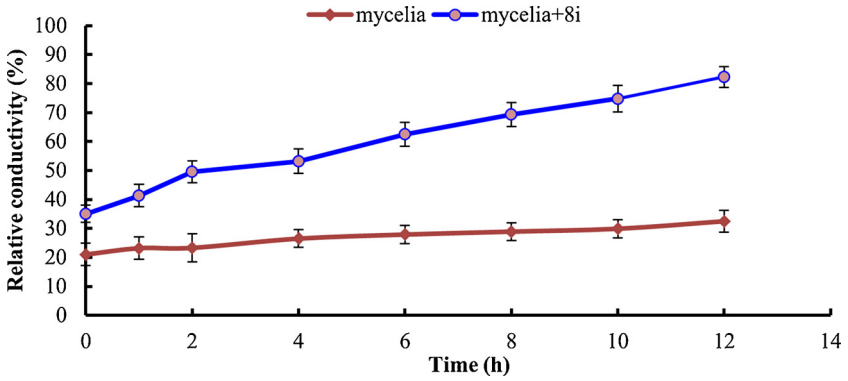

Fig. 3. Mycelial relative conductivity of *T. cucumeris* in the presence or absence of MRA-based acyl-thiourea (8i). Values are mean ± standard error.

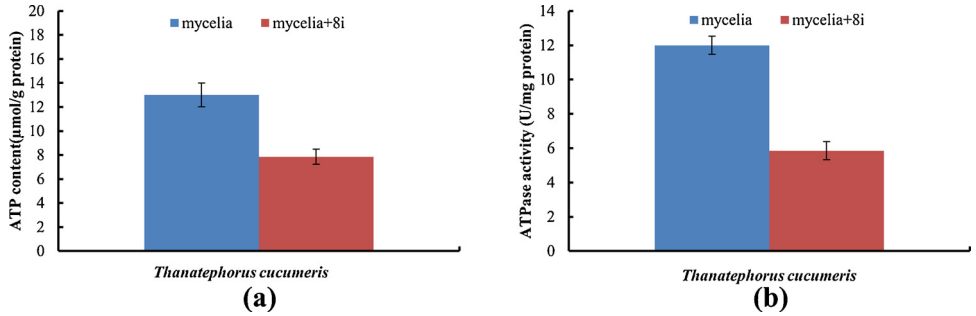

Fig. 4. ATP levels and ATPase activities of mycelia of *T. cucumeris* incubated with or without MRA-based acyl-thiourea (8i). (a) ATP levels; (b) ATPase activities. Values are mean ± standard error.

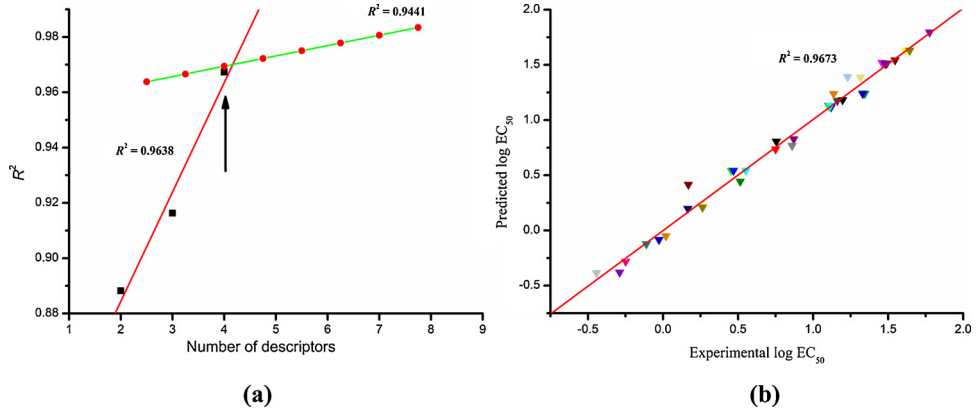

Fig. 5. Determination of the number of descriptors that affect antifungal activity against *T. cucumeris* and antifungal activity prediction using the constructed model. (a) The "breaking point" rule; (b) Experimental and predicted log EC_{50} values.

Table 2
The best four-descriptor model.

ORDescriptor No.	*X*	± *ΔX*	*t*-Test	Descriptor
0	7.3243e + 00	1.6077e + 00	4.5559	Intercept
1	1.6943e + 00	2.6667e-01	−6.3537	q^{S}_{max}
2	−2.2015e + 01	4.6247e + 00	−4.7603	*HOMO-LUMO*
3	−2.1582e + 00	4.2751e-01	5.0483	log *MS*
4	1.1183e + 02	1.1092e + 01	−10.0824	q^{N}_{max}

[a]Maximum net atomic charge for an S atom. b Energy gap between the highest occupied molecular orbit and the lowest unoccupied orbit in atomic units. c Molecular surface area. d Maximum net atomic charge for an N atom.

Table 3
Training and validation set results.

Training set *N*					Test set *N*			
	R^2	*F*	S^2			R^2	*F*	S^2
A + B	27	0.9501	140.26	0.013	C	13	0.9540	132.34 0.017
B + C	26	0.9629	115.84	0.018	A	14	0.9531	125.02 0.019
A + C	27	0.9489	138.1	0.014	B	13	0.9520	125.57 0.018
Average		0.9539	131.4	0.015	Average		0.9530	127.64 0.018

and R^2_{Test} comparable to the overall R^2. The "leave-one-out" cross-validation method was used to assess multiple terpene-based acyl-thiourea analogues, including **7d**, **7 h**, **8b**, **8f**, **8 j**, **13d**, **13 h**, **14b**, **14f** and **14 j**, assigned to the external validation set; the remaining 30 compounds constituted the training set, in which correlation coefficient for the model with identical descriptors was R^2 = 0.9668. R^2 for the latter model in the test set was 0.9697. These findings indicate a

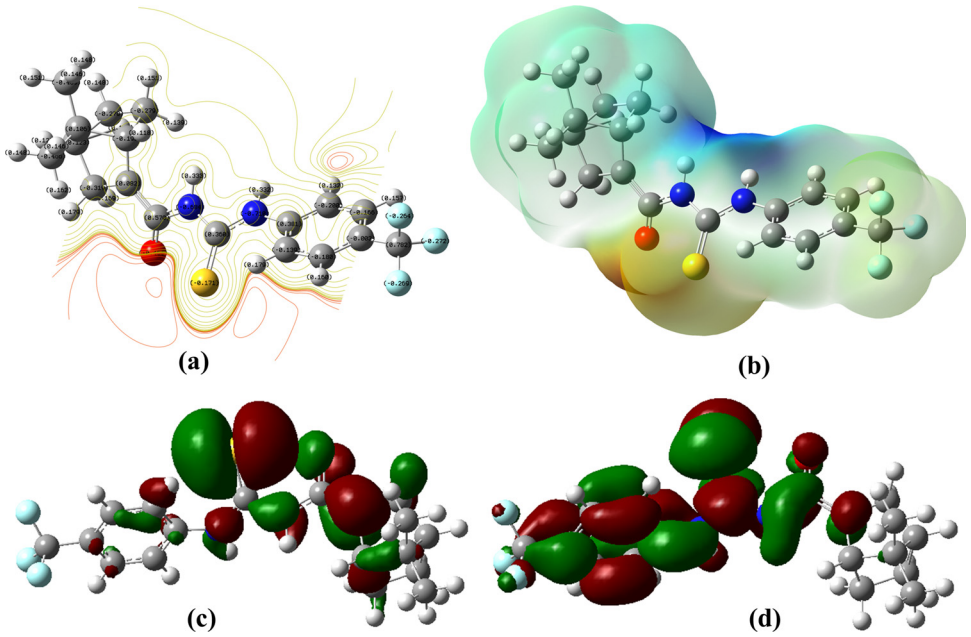

Fig. 6. Charge distribution and energy difference of MRA-based acyl-thiourea (8i) from DFT calculation of Gaussian 16 W. (a) contour map; (b) MEP plot; (c) HOMO energy map; (d) LUMO energy map. Green represents positive molecular orbital, and red parts represents negative molecular orbital. (For interpretation of the references to colour in this figure legend, the reader is referred to the web version of this article.)

satisfactory predictive power for the current QSAR model.

Antifungal activity was predicted by using the constructed model, and predicted results are shown in **Table A. 2**. Meanwhile, deviations between experimental and predicted log EC_{50} values pointed to a reliable model. Fig. 5**b** depicts a comparative analysis of the predicted and experimental activities of 40 terpene-based acyl-thiourea analogues.

Structural properties of terpene-based acyl-thiourea compounds affecting antifungal effects might surface by examining the descriptors found in the generated QSAR model. The 4 leading descriptors were max net atomic charge for an S atom (q^{S}_{max}), energy gap between the highest occupied molecular orbit and the lowest unoccupied orbit in atomic units (*HOMO-LUMO*), molecular surface area (*MS*) and max net atomic charge for an N atom (q^{N}_{max}). The q^{S}_{max} and q^{N}_{max} descriptors are electrostatic, and modulate the antifungal activity against *T. cucumeris* possibly through the thiourea (C = S—NH) group (Crank et al., 1973). As electrostatic activity differs between atoms, the permanent polarization was depicted in the molecular electrostatic potential map (Fig. 6b). Therefore, the nitrogen (NH) and sulfur (C═S) heteroatoms might bind the mycelium at the target site (Abbas et al., 2013). In addition, the contour map of the lead chemical showed that elevated electron density around the substituents attached to nitrogen and sulfur in the terpene-based backbone structure promotes antifungal activity (Fig. 6a). The above findings indicated the electrostatic features of nitrogen and sulfur are an integral component in designing novel and potent antifungals. Electrostatic descriptors thus altered the antifungal properties of test compounds as previously suggested (Saiz-Urra et al., 2009; Lu et al., 2015).

Another critical descriptor was molecular surface area, which is known to be involved in antifungal activity (Siwek et al., 2012; Fan et al., 2018; Lino et al., 2018). Based on previous quantitative structure-activity relationship results, big surface areas would prevent antifungals to reach target sites and alter the ability to interact with cell chemoreceptors; smaller volumes are beneficial to antifungal activity against *T. cucumeris* (Siwek et al., 2012). Here, surface area represented a significant descriptor in the final model, indicating that repellents and the receptor are bound based on surface contact in biological processes, corroborating Sivakumar Ponnurengam et al (Sivakumar Ponnurengam et al., 2009) and Hoque et al (Hoque et al., 2015).

Generally, the *HOMO-LUMO* energy gap, an important descriptor, is broadly employed to assess chemical reactivity; the bigger the gap, the larger the excitation energy and the higher the stability (Fig. 6**c and d**) (Latha et al., 2018). HOMO and LUMO energies, respectively measuring nucleophilicity and electrophilicity, are critical factors in describing electron donating/accepting power, which is consistent with ATP amount and ATPase activity data (Méndez-Hernández et al., 2013; Teunissen et al., 2017). Based on the above results, we speculated that the energy features of molecules might be critical for their antifungal activities, and fungicides with higher efficacy should be active and promote electrophilic interactions with the receptor.

Above all, according to the requirement of ecological agriculture, both food safety and disease prevention are considerable issues. Through this study, some new antifungal drugs of novel structure, low cost and high efficient activity were prepared, which provided kind of new idea for integrated pest management of modern agriculture.

4. Conclusions

In this study, four series of terpene-based acyl-thiourea derivatives, namely **7a-j**, **8a-j**, **13a-j** and **14a-j**, were synthesized, with their antifungal activities against *B. cinerea*, *S. sclerotiorum* and *T. cucumeris* evaluated. Turpentine-based compounds exhibited obviously higher activities compared with rosin-based counterparts with the same substitution group, especially the MRA-based acyl-thiourea compound (**8i**), which had a lower EC_{50} value compared with carbendazim. Similarly, *in vivo* the antifungal efficiency against *T. cucumeris* of **8i** was excellent. In physiological and biochemical response assessment of **8i**, mycelial morphology was affected obviously, with cell membrane permeability increased remarkably, reduced ATP amounts and ATPase activity, in comparison with control values. QSAR and SAR studies demonstrated that elevated electron density around the substituents on nitrogen and sulfur in terpene-based acyl-thiourea compounds, reduced spatial volume, and HOMO and LUMO energy difference are beneficial for antifungal activity. Enlightened by this conclusion, we considered the following work to synthesize some efficient terpene-based acyl-thiourea fungicides with electron-withdrawing substituents such as halogen group and smaller volume of spatial structure. These findings provide critical insights into the modes of action of terpene-based acyl-thiourea derivatives and would help develop novel natural product-based antifungal agents.

Acknowledgments

This work was supported by the National Key R&D Program of China (grant number 2018YFD0600402), the National Natural Science Foundation of China (grant number 31870555), and the Young Talent Cultivation Plan of Northwest A&F University (grant number 2452018031).

Appendix A. Supplementary data

Supplementary material related to this article can be found, in the online version, at doi:https://doi.org/10.1016/j.indcrop.2018.10.008.

References

Abbas, S.Y., El-Sharief, M.A.M.S., Basyouni, W.M., Fakhr, I.M.I., El-Gammal, E.W., 2013. Thiourea derivatives incorporating a hippuric acid moiety: synthesis and evaluation of antibacterial and antifungal activities. Eur. J. Med. Chem. 64, 111–120.

Baba, A., Yoshioka, T., 2009. Structure−activity relationships for the degradation reaction of 1-β-O-acyl glucuronides. Part 3: Electronic and steric descriptors predicting the reactivity of aralkyl carboxylic acid 1-β-O-acyl glucuronides. Chem. Res. Toxicol. 22, 1998–2008.

Berben, P., Bauer-Brandl, A., Brandl, M., Faller, B., Flaten, G.E., Jacobsen, A.C., Brouwers, J., Augustijns, P., 2018. Drug permeability profiling using cell-free permeation tools: overview and applications. Chem. Res. Toxicol. 119, 219–233.

Burgeson, J.R., Moore, A.L., Boutilier, J.K., Cerruti, N.R., Gharaibeh, D.N., Lovejoy, C.E., Amberg, S.M., Hruby, D.E., Tyavanagimatt, S.R., Allen, R.D., Dai, D., 2012. SAR analysis of a series of acylthiourea derivatives possessing broad-spectrum antiviral activity. Bioorg. Med. Chem. Lett. 22, 4263–4272.

Crank, G., Neville, M., Ryden, R., 1973. Thiourea derivatives of 2-aminooxazoles showing antibacterial and antifungal activity. J. Med. Chem. 16, 1402–1405.

Curtin, M.L., Heyman, H.R., Clark, R.F., Sorensen, B.K., Doherty, G.A., Hansen, T.M., Frey, R.R., Sarris, K.A., Aguirre, A.L., Shrestha, A., Tu, N., Woller, K., Pliushchev, M.A., Sweis, R.F., Cheng, M., Wilsbacher, J.L., Kovar, P.J., Guo, J., Cheng, D., Longenecker, K.L., Raich, D., Korepanova, A.V., Soni, N.B., Algire, M.A., Richardson, P.L., Marin, V.L., Badagnani, I., Vasudevan, A., Buchanan, F.G., Maag, D., Chiang, G.G., Tse, C., Michaelides, M.R., 2017. SAR and characterization of non-substrate isoindoline urea inhibitors of nicotinamide phosphoribosyltransferase (NAMPT). Bioorg. Med. Chem. Lett. 27, 3317–3325.

Deb, T., Anderson, C.M., Chattopadhyay, S., Ma, H., Young, V.G., Jensen, M.P., 2014. Steric and electronic effects on arylthiolate coordination in the pseudotetrahedral complexes [(TpPh,Me)Ni-SAr] (TpPh,Me = hydrotris{3-phenyl-5-methyl-1-pyrazolyl}borate). Dalton Trans. 43, 17489–17499.

Fan, Z., Qin, Y., Liu, S., Xing, R., Yu, H., Chen, X., Li, K., Li, P., 2018. Synthesis, characterization, and antifungal evaluation of diethoxyphosphoryl polyaminoethyl chitosan derivatives. Carbohyd. Polym. 190, 1–11.

Gao, H., Chen, S., Rao, X., Shang, S., Song, Z., 2013. A new dehydroabietic acid-based arylamine fluorescent probe: synthesis, structure analysis and in vitro biodiagnose function. Bioorg. Med. Chem. Lett. 23, 2254–2259.

Gao, Y., Li, L., Chen, H., Li, J., Song, Z., Shang, S., Song, J., Wang, Z., Xiao, G., 2015. High value-added application of rosin as a potential renewable source for the synthesis of acrylopimaric acid-based botanical herbicides. Ind. Crop. Prod. 78, 131–140.

Haynes, C.J.E., Busschaert, N., Kirby, I.L., Herniman, J., Light, M.E., Wells, N.J., Marques, I., Felix, V., Gale, P.A., 2014. Acylthioureas as anion transporters: the effect of intramolecular hydrogen bonding. Org. Biomol. Chem. 12, 62–72.

Hoque, J., Akkapeddi, P., Yadav, V., Manjunath, G.B., Uppu, D.S.S.M., Konai, M.M., Yarlagadda, V., Sanyal, K., Haldar, J., 2015. Broad spectrum antibacterial and antifungal polymeric paint materials: synthesis, structure–activity relationship, and membrane-active mode of action. ACS Appl. Mater. Int. 7, 1804–1815.

James Bound, D., Murthy, P.S., Srinivas, P., 2016. 2,3-Dideoxyglucosides of selected terpene phenols and alcohols as potent antifungal compounds. Food Chem. (210), 371–380.

Jenkins, I.D., Lacrampe, F., Ripper, J., Alcaraz, L., Van Le, P., Nikolakopoulos, G., de Almeida Leone, P., White, R.H., Quinn, R.J., 2008. Synthesis of four novel natural product inspired scaffolds for drug discovery. J. Org. Chem. 74, 1304–1313.

Jing, L., Lei, Z., Li, L., Xie, R., Xi, W., Guan, Y., Sumner, L.W., Zhou, Z., 2014. Antifungal activity of citrus essential oils. J. Agric. Food Chem. 62, 3011–3033.

Joshi, R., Pandey, N., Yadav, S.K., Tilak, R., Mishra, H., Pokharia, S., 2018. Synthesis, spectroscopic characterization, DFT studies and antifungal activity of (E)-4-amino-5-[N'-(2-nitro-benzylidene)-hydrazino]-2,4-dihydro-[1,2,4]triazole-3-thione. J. Mol. Struct. (1164), 386–403.

Kiyama, R., 2017. Estrogenic terpenes and terpenoids: pathways, functions and applications. Eur. J. Pharmacol. 815, 405–415.

Latha, B., Kumaresan, P., Nithiyanantham, S., Sampathkumar, K., 2018. HOMO-LUMO analysis of multi walled carbon nanotubes doped tetrafluoro phthalate crystals for nonlinear optical applications. J. Mol. Struct. 1152, 351–360.

Li, J., Li, J., Gao, Y., Shang, S., Song, Z., Xiao, G., 2016. Taking advantage of a sustainable forest resource in agriculture: a value-added application of volatile turpentine analogues as botanical pesticides based on amphipathic modification and QSAR study. ACS Sustain. Chem. Eng. 4, 4685–4691.

Liao, S., Liu, Y., Si, H., Xiao, Z., Fan, G., Chen, S., Wang, P., Wang, Z., 2017. Hydronopylformamides: modification of the naturally occurring compound (-)-β-pinene to produce insect repellent candidates against blattella germanica. Molecules 22, 1004–1011.

Lino, C.I., Gonçalves de Souza, I., Borelli, B.M., Silvério Matos, T.T., Santos Teixeira, I.N., Ramos, J.P., Maria de Souza Fagundes, E., de Oliveira Fernandes, P., Maltarollo, V.G., Johann, S., de Oliveira, R.B., 2018. Synthesis, molecular modeling studies and evaluation of antifungal activity of a novel series of thiazole derivatives. Eur. J. Med. Chem. 151, 248–260.

Lu, A., Ma, Y., Wang, Z., Zhou, Z., Wang, Q., 2015. Application of "hydrogen-bonding interaction" in drug design. Part 2: Design, synthesis, and structure–activity relationships of thiophosphoramide derivatives as novel antiviral and antifungal agents. J. Agr. Food Chem. 63, 9435–9440.

Lv, J., Zhang, B.B., Liu, X.D., Zhang, C., Chen, L., Xu, G.R., Cheung, P.C.K., 2017. Enhanced production of natural yellow pigments from monascus purpureus by liquid culture: the relationship between fermentation conditions and mycelial morphology. J. Biosci. Bioeng. 124, 452–458.

Manetti, F., Taddei, M., Petricci, E., 2015. Structure–activity relationships and mechanism of action of small molecule smoothened modulators discovered by high-throughput screening and rational design. In: Ruat, M. (Ed.), The Smoothened Receptor in Cancer and Regenerative Medicine. Springer International Publishing. Cham, pp. 43–107.

Méndez-Hernández, D.D., Tarakeshwar, P., Gust, D., Moore, T.A., Moore, A.L., Mujica, V., 2013. Simple and accurate correlation of experimental redox potentials and DFT-calculated HOMO/LUMO energies of polycyclic aromatic hydrocarbons. J. Mol. Model. 19, 2845–2848.

Ntalli, N.G., Ferrari, F., Giannakou, I., Menkissoglu-Spiroudi, U., 2010. Phytochemistry and nematicidal activity of the essential oils from 8 Greek lamiaceae aromatic plants and 13 terpene components. J. Agr. Food Chem. 58, 7856–7863.

Papa, E., Kovarich, S., Gramatica, P., 2010. QSAR modeling and prediction of the endocrine-disrupting potencies of brominated flame retardants. Chem. Res. Toxicol. 23, 946–954.

Quin, M.B., Flynn, C.M., Schmidt-Dannert, C., 2014. Traversing the fungal terpenome. Nat. Prod. Rep. 31, 1449–1473.

Saiz-Urra, L., Racero, J.C., Macías-Sánchez, A.J., Hernández-Galán, R., Hanson, J.R., Perez-Gonzalez, M., Collado, I.G., 2009. Synthesis and quantitative structure−-antifungal activity relationships of clovane derivatives against botrytis cinerea. J. Agr. Food Chem. 57, 2420–2428.

Schwamborn, M., Schumacher, J., Sibold, J., Teiwes, N.K., Steinem, C., 2017. Monitoring ATPase induced pH changes in single proteoliposomes with the lipid-coupled fluorophore Oregon green 488. Analyst 142, 2670–2677.

Sekiya, M., Shimoyama, Y., Ishikawa, T., Sasaki, M., Futai, M., Nakanishi-Matsui, M., 2018. Porphyromonas gingivalis is highly sensitive to inhibitors of a proton-pumping ATPase. Biochem. Bioph. Res. Co. 498, 837–841.

Shao, W., Zhang, Y., Ren, W., Chen, C., 2015. Physiological and biochemical characteristics of laboratory induced mutants of botrytis cinerea with resistance to fluazinam. Pestic. Biochem. Phys. 117, 19–23.

Sivakumar Ponnurengam, M., Muthu Kumar, T., Doble, M., 2009. Antifungal activity, mechanism and QSAR studies on chalcones. Chem. Biol. Drug Des. 74, 68–79.

Siwek, A., Stefańska, J., Dzitko, K., Ruszczak, A., 2012. Antifungal effect of 4-arylthiosemicarbazides against Candida species. Search for molecular basis of antifungal activity of thiosemicarbazide derivatives. J. Mol. Model. 18, 4159–4170.

Sklenar, J., Fox, G.G., Loughman, B.C., Pannifer, A.D.B., Ratcliffe, R.G., 1994. Effects of vanadate on the ATP content, ATPase activity and phosphate absorption capacity of maize roots. Plant Soil 167, 57–62.

Smith, G.H., Roberts, J.M., Pope, T.W., 2018. Terpene based biopesticides as potential alternatives to synthetic insecticides for control of aphid pests on protected ornamentals. Crop Prot. 110, 125–130.

Solinas, A., Faure, H., Roudaut, H., Traiffort, E., Schoenfelder, A., Mann, A., Manetti, F., Taddei, M., Ruat, M., 2012. Acylthiourea, acylurea, and acylguanidine derivatives with potent hedgehog inhibiting activity. J. Med. Chem. 55, 1559–1571.

Song, J., Wang, Z., Findlater, A., Han, Z., Jiang, Z., Chen, J., Zheng, W., Hyde, S., 2013. Terpenoid mosquito repellents: a combined DFT and QSAR study. Bioorg. Med. Chem. Lett. 23, 1245–1248.

Sparks Thomas, C., Hahn Donald, R., Garizi Negar, V., 2016. Natural products, their derivatives, mimics and synthetic equivalents: role in agrochemical discovery. Pest Manag. Sci. 73, 700–715.

Sun, C., Huang, H., Feng, M., Shi, X., Zhang, X., Zhou, P., 2006. A novel class of potent influenza virus inhibitors: polysubstituted acylthiourea and its fused heterocycle derivatives. Bioorg. Med. Chem. Lett. 16, 162–166.

Teunissen, J.L., De Proft, F., De Vleeschouwer, F., 2017. Tuning the HOMO–LUMO energy gap of small diamondoids using inverse molecular design. J. Chem. Theory Comput. 13, 1351–1365.

Thiehoff, C., Schifferer, L., Daniliuc, C.G., Santschi, N., Gilmour, R., 2016. The influence of electronic perturbations on the sulfur–fluorine gauche effect. J. Fluorine Chem. 182, 121–126.

Tsuchikawa, H., Hayashi, T., Shibata, H., Murata, M., Nagumo, Y., Usui, T., 2016. Bafilomycin analogue site-specifically fluorinated at the pharmacophore macrolactone ring has potent vacuolar-type ATPase inhibitory activity. Tetrahedron Lett. 57, 2426–2429.

Vraćko, M., Szymoszek, A., Barbieri, P., 2004. Structure-mutagenicity study of 12 trimethylimidazopyridine isomers using orbital energies and "spectrum-like representation" as descriptors. J. Chem. Inf. Comp. Sci. 44, 352–358.

Wang, M.J., Nan, X., Feng, G., Yu, H.T., Hu, G.F., Liu, Y.Q., 2014. Design, synthesis and bioactivity evaluation of novel acylthiourea derivatives of cantharidin. Ind. Crop. Prod. 55, 11–18.

Wright, A.D., Wang, H., Gurrath, M., König, G.M., Kocak, G., Neumann, G., Loria, P.,

Foley, M., Tilley, L., 2001. Inhibition of heme detoxification processes underlies the antimalarial activity of terpene isonitrile compounds from marine sponges. J. Med. Chem. 44, 873–885.
Yang, M., Wang, G., 2016. ATPase activity measurement of DNA replicative helicase from Bacillus stearothermophilus by malachite green method. Anal. Biochem. 509, 46–49.
Yang, D., Wan, C., He, M., Che, C., Xiao, Y., Fu, B., Qin, Z., 2017. Design, synthesis, crystal structure and fungicidal activity of (E)-5-(methoxyimino)-3,5-dihydrobenzo[e][1,2] oxazepin-4(1H)-one analogues. Med. Chem. Comm. 8 1007–1014.
Yoshioka, T., Baba, A., 2009. Structure – activity relationships for the degradation reaction of 1-β-O-acyl glucuronides. Part 2: electronic and steric descriptors predicting the reactivity of 1-β-O-acyl glucuronides derived from benzoic acids. Chem. Res. Toxicol. 22, 1559–1569.
Yu, X., Teng, P., Zhang, Y.L., Xu, Z.J., Zhang, M.Z., Zhang, W.H., 2018. Design, synthesis and antifungal activity evaluation of coumarin-3-carboxamide derivatives. Fitoterapia 127, 387–395.
Yun, Y.Z., Liu, Z.Y., Yin, Y.N., Jiang, J.H., Chen, Y., Xu, J.R., Ma, Z.H., 2015. Functional analysis of the Fusarium graminearum phosphatome. New Phytol. 207, 119–134.
Yun, T., Qin, T., Liu, Y., Lai, L., 2016. Identification of acylthiourea derivatives as potent Plk1 PBD inhibitors. Eur. J. Med. Chem. 124, 229–236.
Zhang, J.F., Xu, J.Y., Wang, B.L., Li, Y.X., Xiong, L.X., Li, Y.Q., Ma, Y., Li, Z.M., 2012. Synthesis and insecticidal activities of novel anthranilic diamides containing acylthiourea and acylurea. J. Agric. Food Chem. 60, 7565–7572.
Zhang, H., Bai, L., He, J., Zhong, L., Duan, X., Ouyang, L., Zhu, Y., Wang, T., Zhang, Y., Shi, J., 2017. Recent advances in discovery and development of natural products as source for anti-Parkinson's disease lead compounds. Eur. J. Med. Chem. 141, 257–272.
Zhao, C., Kim, Y., Zeng, Y., Li, M., Wang, X., Hu, C., Gorman, C., Dai, S.Y., Ding, S.-Y., Yuan, J.S., 2018. Co-compartmentation of terpene biosynthesis and storage via synthetic droplet. ACS Synth. Biol. 7, 774–781.